Published in final edited form as:
Bull Am Meteorol Soc. 2017 June ; 98(6): 1185–1198. doi:10.1175/bams-d-16-0019.1.

PDRMIP: A Precipitation Driver and Response Model Intercomparison Project, Protocol and preliminary results

G. Myhre,
CICERO Center for International Climate and Environmental Research – Oslo, Norway

P. M. Forster,
University of Leeds, Leeds, United Kingdom

B. H. Samset,
CICERO Center for International Climate and Environmental Research – Oslo, Norway

Ø. Hodnebrog,
CICERO Center for International Climate and Environmental Research – Oslo Norway

J. Sillmann,
CICERO Center for International Climate and Environmental Research – Oslo, Norway

S. G. Aalbergsjø,
CICERO Center for International Climate and Environmental Research – Oslo, Norway

T. Andrews,
Met Office Hadley Centre, Exeter, UK

O. Boucher,
Laboratoire de Météorologie Dynamique, IPSL, Univ. P et M. Curie / CNRS, Paris, France

G. Faluvegi,
Columbia University, New York, USA

D. Fläschner,
Max-Planck-Institut fur Meteorologie, Hamburg Germany

T. Iversen,
Norwegian Meteorological Institute, Oslo, Norway

M. Kasoar,
Imperial College London, London, United Kingdom

V. Kharin,
Canadian Centre for Climate Modelling and Analysis, Victoria, BC, Canada A. Kirkevåg,
Norwegian Meteorological Institute, Oslo, Norway

J.-F. Lamarque,

Corresponding Author: G. Myhre, CICERO Center for International Climate and Environmental Research – Oslo, Post Office Box 1129 Blindern, N-0318 Oslo, Norway gunnar.myhre@cicero.oslo.no.

PDRMIP investigates the role of various drivers of climate change for mean and extreme precipitation changes, based on multiple climate model output and energy budget analyses.

NCAR/UCAR, Boulder, USA

D. Olivié,
Norwegian Meteorological Institute, Oslo, Norway

T. Richardson,
University of Leeds, United Kingdom

D. Shindell,
Duke University, Durham, USA

K. P. Shine,
University of Reading, Reading, United Kingdom

Camilla W. Stjern,
CICERO Center for International Climate and Environmental Research – Oslo, Norway

T. Takemura,
Kyushu University, Fukuoka, Japan

A. Voulgarakis,
Imperial College London, London, United Kingdom

F. Zwiers
Pacific Climate Impacts Consortium University of Victoria, Canada

Abstract

As the global temperature increases with changing climate, precipitation rates and patterns are affected through a wide range of physical mechanisms. The globally averaged intensity of extreme precipitation also changes more rapidly than the globally averaged precipitation rate. While some aspects of the regional variation in precipitation predicted by climate models appear robust, there is still a large degree of inter-model differences unaccounted for. Individual drivers of climate change initially alter the energy budget of the atmosphere leading to distinct rapid adjustments involving changes in precipitation. Differences in how these rapid adjustment processes manifest themselves within models are likely to explain a large fraction of the present model spread and needs better quantifications to improve precipitation predictions. Here, we introduce the Precipitation Driver and Response Model Intercomparison Project (PDRMIP), where a set of idealized experiments designed to understand the role of different climate forcing mechanisms were performed by a large set of climate models. PDRMIP focuses on understanding how precipitation changes relating to rapid adjustments and slower responses to climate forcings are represented across models. Initial results show that rapid adjustments account for large regional differences in hydrological sensitivity across multiple drivers. The PDRMIP results are expected to dramatically improve our understanding of the causes of the present diversity in future climate projections.

Introduction

Changes to both mean and extreme precipitation have been observed over the last century, due partly to global warming, and changes are expected to become more marked over this century (Stocker et al. 2013). Human society is vulnerable to changes in precipitation, because of the importance of precipitation for fresh water availability and food production, but also because of potential damages to infrastructure caused by extreme precipitation. Robust changes in regional precipitation patterns have been found across current Coupled Model Intercomparison Project Phase 5 (CMIP5) climate models for the industrial era and future climate, such as a drying in many sub-tropical regions and enhanced precipitation at high latitudes. However, the diversity among the CMIP5 models is large both in terms of global mean and regional predicted precipitation change (Knutti and Sedlacek 2013). Furthermore evaluation of the current generation of climate models reveals precipitation biases (Flato et al. 2013; Mehran et al. 2014). Extensive studies have been performed on how precipitation responds to climate change using observations and modelling (e.g. Trenberth (2011)), but significant questions still remain, particularly with respect to dynamical changes on precipitation (Muller and O'Gorman 2011).

The precipitation at a particular location is highly variable and depends on local and actual weather conditions. However, on a global scale, precipitation is strongly constrained by the energy budget within the climate system (Mitchell et al. 1987; Allen and Ingram 2002; Stephens et al. 2012) and is described in more detail in Box 1.

The energy budget is altered by both natural and anthropogenic influences. Depending on the physical properties of a climate forcing mechanism, it causes either a fast response in precipitation, on timescales of days to weeks, or a slower response on a timescale of years (Andrews et al. 2010; Ming et al. 2010; Frieler et al. 2011; Pendergrass and Hartmann 2012), or both (see Box Figure 1). Bala et al. (2010) suggested that multi-model comparisons should be constructed such that fast and slow precipitation responses could be separately evaluated. It has been shown in several model studies that the global mean, fast atmospheric response correlates strongly with the atmospheric component of radiative forcing, while the slower response scales with global surface temperature change (Andrews et al. 2010; Kvalevåg et al. 2013) which has a long time scale due to the large thermal capacity of the ocean. Figure 1 illustrates these fast and slow precipitation changes for various drivers of climate change from two climate models (Andrews et al. 2010; Kvalevåg et al. 2013) combined with the new PDRMIP results (Samset et al. 2016).

On regional scales the fast precipitation response is more complex due to changes in atmospheric circulation. Rapid circulation changes in response to forcing are associated with the change in atmospheric absorption (Bony et al. 2013; Merlis 2015) as well as the rapid land surface response (Shaw and Voigt 2015; Richardson et al. 2016). Land surface temperature responds on very short time-scales and can drive significant shifts in tropical convection and precipitation (Dong et al. 2014). As a result, climate drivers such as sulphate aerosols or changes in the solar constant, which have small effects on atmospheric absorption, can still produce rapid spatial shifts in precipitation due to the surface forcing. Heterogeneity of radiative forcings (e.g. sulphate and black carbon (BC)) will also lead to distinct regional precipitation responses through changes in atmospheric circulation. Further descriptions of rapid adjustments, which includes the fast precipitation changes caused by atmospheric absorption, are discussed by Boucher et al. (2013); Myhre et al. (2013a); Sherwood et al. (2015).

The drivers of climate change included in Figure 1 span a wide range of agents for atmospheric absorption, causing different rapid adjustments as well as slower responses from surface temperature change. Ming et al. (2010); Kvalevåg et al. (2013) found a strong dependence of the fast response on the location of BC concentration with height. For ozone forcing changes, Andrews et al. (2010) found both fast and slow precipitation responses to be small, but recently Macintosh et al. (2016) found that for the industrial era, fast precipitation response from ozone changes is also strongly dependent on the altitude of the ozone change. Stratospheric aerosols are also found to give a fast precipitation response (Ferraro and Griffiths 2016). Flaschner et al. (2016) showed that accounting for differences in the fast precipitation response explains much of the previously reported large variation in hydrological sensitivity (change in global mean precipitation per global mean temperature change) between climate models. The estimated factor of 3 spread in the hydrological sensitivity (Held and Soden 2006; Previdi 2010; Pendergrass and Hartmann 2014) can be reduced to an inter-model spread of 1.5 when the diversity in rapid adjustment is corrected for (Fläschner et al. 2016). An additional source of spread in hydrological sensitivity has been identified as inter-model differences in the representation of absorption of shortwave radiation relating to the representation of radiative transfer by water vapor (e.g. Takahashi (2009); DeAngelis et al. (2015); Fildier and Collins (2015)). This enhanced atmospheric absorption, as water vapor concentrations increase, is conceptually similar to the drivers of fast precipitation change, but since the water vapor change is driven by feedbacks on the global energy budget, it is better viewed as part of the slow response.

The rates of extreme precipitation events have been found, both through observations and modelling, to scale closely with the Clausius-Clapeyron relationship rather than with global mean precipitation change (Allan and Soden 2008; Boucher et al. 2013; O'Gorman 2015). This is supported by several CMIP5 studies (e.g., Kharin et al. (2013); Sillmann et al. (2013b); Pendergrass et al. (2015)) which indicate that increases in globally averaged extreme precipitation are about three times as large as the increase in mean precipitation under different greenhouse gas emission scenarios. The scaling of extreme precipitation with temperature may however be much more complex than what is implied by the Clausius-Clapeyron relationship, with considerable regional variations due to various dynamic and thermodynamic mechanisms (e.g., Caesar and Lowe (2012); Westra et al. (2013)). From the CMIP5 ensemble, the increase in 20-year return values of the annual extremes of daily precipitation is estimated to be about 6%/K, with a large inter-model range between 4%-10%/K according to Kharin et al. (2013). This considerable uncertainty in estimates of the of the Clausius-Clapeyron relationship for extreme precipitation compared to mean precipitation is most pronounced in the tropics. The physical understanding of this larger increase in extreme precipitation per global temperature change is based on the fact that relative humidity is expected, both from observations and climate models, to be approximately constant in a warmer climate. Water vapor content in the lower atmosphere will therefore increase by 6-7% per K of warming, thus providing more water available for intense precipitation events. Furthermore, there are indications both from observations and modelling studies, that sub-daily (or hourly) extreme precipitation may increase even faster than suggested by the Clausius-Clapeyron relationship (Lenderink and Van Meijgaard 2008; Berg et al. 2013; Kendon et al. 2014; Westra et al. 2014). However, this has recently been questioned and could be related to sampling issues (Ban et al. 2015). Recent findings nonetheless indicate that changes in the storms dynamics may result in precipitation changes that are greater than those implied by the Clausius-Clapeyron relationship (Wasko et al. 2016). Different drivers of climate change may impact the extreme precipitation differently and Sillmann et al. (2013a) found a relatively large impact of aerosols reductions on climate extremes over Europe in a climate model.

The range in atmospheric absorption associated with the drivers of climate change is important for understanding precipitation changes and the associated model diversity, as illustrated in Figure 1. However, no dedicated model intercomparison project has previously been undertaken, leaving open the question of whether rapid adjustments are indeed similarly represented across models with respect to precipitation changes. We present here PDRMIP (http://www.cicero.uio.no/en/PDRMIP), an open, international study designed to extend the analysis of the impacts of single precipitation drivers, on short and long time scales, to a broad range of climate models. The aim of PDRMIP is to perform a thorough investigation of differences in the effects of anthropogenic and natural drivers on precipitation and extreme precipitation events. This will be accomplished based on five core simulations, with global perturbation to either anthropogenic or natural drivers of climate change, as well as six selected regional perturbation experiments.

PDRMIP will in particular enhance the understanding of drivers of climate change other than CO_2 on cloud changes, climate sensitivity, and precipitation including extremes. At present a wide range of forcing mechanisms contribute to climate change (Forster et al. 2007; Myhre et al. 2013a). The efficacy of different drivers of climate change to change the surface temperature from a radiative forcing perturbation has been compared to CO_2 in individual models (Hansen et al. 2005; Yoshimori and Broccoli 2008); in PDRMIP, this will be performed in a large set of climate models. The focus is on the global climate perspective, with additional work examining changes in precipitation over land versus ocean, and over key regions of the globe. Since most of the analysis of PDRMIP has been performed ahead of completion of the ongoing CMIP6 exercise, the results will greatly contribute to understanding aspects of the CMIP6 results.

Experimental design

PDRMIP asks modelling groups to perform one baseline and five core perturbation experiments, complemented by to six regional simulations, in order to explore the responses to climate drivers occurring in different regions, which have been suggested to vary strongly (Shindell et al. 2012). The core experiments consist of simulations with a doubling of CO_2 concentration, tripling of CH_4 concentration, a 2% increase in total solar irradiance, and two experiments increasing the anthropogenic aerosol concentrations, see Table 1. The additional simulations are dedicated to regional changes in aerosols and ozone, the climate drivers that feature strong spatial variability (see Table 2). These simulations are related to the large increase in aerosols and their precursors over South East Asia over the last decades and potential mitigation efforts.

NASA Author Manuscript

NASA Author Manuscript

For models where it is possible to prescribe aerosol concentration fields, PDRMIP provides a common set of baseline and perturbed concentrations. This is done in order to minimize the effect on the results from differences in geographical and vertical aerosol distributions in the models. It is known that despite identical aerosol fields, the forcing will differ due to varying complexities in aerosol-radiation and aerosol-cloud interactions, as well as host model differences (Stier et al. 2013). This is therefore also likely a cause for inter-model variability in precipitation change estimates. The baseline PDRMIP aerosol fields are constructed from the multi-model mean from AeroCom Phase II, see Figure 2. Models that are only able to drive aerosol fields through emissions will instead scale their native emission fields. Even though this introduces additional variability in the results, it is highly preferable to still have these models participate. We note that rapid adjustments associated with climate drivers with significant change in atmospheric radiative cooling, especially CO_2 and black carbon (Boucher et al. 2013; Myhre et al. 2013a; Sherwood et al. 2015), are unavoidably included in the climate model simulations, and the semi-direct cloud effect of black carbon is therefore automatically included in all PDRMIP simulations.

To diagnose both the fast and slow response in precipitation (Andrews et al. 2010; Bala et al. 2010) the model simulations are performed both with fixed sea-surface temperatures (SSTs) and with fully coupled (or slab ocean) configurations of the models. The length of the fixed-SST simulations is a minimum of 15 years and the fully coupled climate simulations are 100 years long. The fast response is derived from the last 10 years of the fixed-SST simulations, and the total response from the last 50 years of the coupled simulations. The slow response is calculated as the fast response subtracted from the total response. The forcing of the climate drivers can be derived both from the fixed-SST TOA fluxes and from the regression of the imbalance in the TOA net radiative fluxes and surface temperature from the coupled simulations (Gregory et al. 2004; Boucher et al. 2013; Myhre et al. 2013a). Additional simulations will be performed by a subset of models to investigate the behaviour of the system beyond 100 years.

The PDRMIP model output is on standardized format from a subset of the CMIP5 output protocol and will be made available for the research community on request, through a Norwegian national data storage facility.

The list of ten PDRMIP models, described in Table 3, includes models that either have been used in CMIP5 or will be used in CMIP6. Some of the ten PDRMIP models are different versions of the same climate models, whereas others are largely independent (Knutti et al. 2013).

General PDRMIP results

Figures 1, 3, 4, and 5 show some overall results from the main PDRMIP simulations. Figure 3 shows zonal mean temperature changes, precipitation changes, radiative forcing, and atmospheric absorption for the five PDRMIP climate drivers. The well-known strong high latitude temperature response, especially in the northern hemisphere, is evident for all five PDRMIP drivers. This is also the case for CH_4 and BC with smaller temperature response than for the other drivers. In relative terms, the precipitation changes are largest at high northern latitudes. However, the tropics has larger absolute precipitation and quite large relative changes are found here, but these changes vary with latitude. Changes in precipitation in the sub-tropics are relatively small for the PDRMIP drivers.

The zonal mean radiative forcing and atmospheric absorption shows that the PDRMIP drivers differ substantially. Of the two drivers mostly affecting longwave radiation, CO_2 has a slightly stronger atmospheric absorption compared to top-of-atmosphere radiative forcing than CH_4 (Samset et al. 2016). The atmospheric absorption in the solar and sulphate experiments is weak (also shown in Figure 1). The corresponding radiative forcings on the other hand differ, with strong forcings in the tropics and the largest difference between the tropics and high latitudes in the solar experiment, whereas in the sulphate experiment the forcing has a maximum in absolute terms around 40°N. In the BC experiment the radiative forcing is relatively weak, but with a very strong atmospheric absorption locally reaching more than 8 W m^{-2} in zonal average.

Figure 4 shows the geographical distribution of multi-model mean apparent hydrological sensitivity (HS) for the five core PDRMIP climate drivers (CO2x2, CH4x3, Solar+2%, BCx10, SO4x5). The apparent HS parameter is calculated as the annual mean geographical precipitation change over the last 50 years of the PDRMIP coupled/slab ocean simulations, divided by global and annual mean temperature change relative to the base simulation. The apparent HS includes both the rapid adjustments to the introduction of a climate driver, and the resulting slow, purely temperature driven response. For the three first drivers, CO_2, CH_4 and solar irradiance, differences in the geographical distribution among the drivers are modest. We find weak or negative sensitivities in sub-tropical regions, and strongly positive sensitivities in tropical regions associated with a strengthened ITCZ, as well as at mid-latitudes.

The apparent HS from an increase in BC differs substantially from that of the other drivers, especially in the sub-tropical regions, with smaller differences around the ITCZ and mid to high latitudes. Unlike the other climate drivers investigated in PDRMIP, the reduced precipitation in sub-tropical regions overwhelms the increase in other regions for BC on a global scale. The contrasting regional precipitation pattern is larger for BC than for the other forcing agents.

The different responses to increasing concentrations of sulphate aerosols compared to responses to solar changes illustrate that the regional pattern of the climate driver also influences the precipitation changes, with a notable shift in the ITCZ and changes over Asia. We find stronger precipitation changes from sulphate aerosols than from greenhouse gases over Asia, similar to earlier findings (Shindell et al. 2012). Note that for an increase in sulphate aerosols the global mean surface temperature change is negative, unlike the other climate drivers in Figure 4. Over land, increased anthropogenic sulphate aerosols have thus generally reduced precipitation such as over equatorial Africa or South Asia, in accordance with previous findings (Bollasina et al. 2011; Hwang et al. 2013).

Earlier studies have found that rapid adjustments have been important for global precipitation change (Andrews et al. 2010; Kvalevåg et al. 2013). Figure 4 and shown in

Samset et al. (2016) Figure 2, implies that the impact of rapid adjustments on regional precipitation changes may be substantial, particularly for BC. Further PDRMIP studies will investigate the inter-model diversity of the hydrological sensitivity and its dependence on forcing agent and location.

Figure 5 shows changes in precipitation extremes as defined in terms of 20-year return values of annual maximum daily precipitation following Kharin et al. (2013). A return value for a specified T-year return period is the value that is exceeded by an annual extreme with probability $p = 1/T$. Hence, a 20-year return period corresponds to an annual exceedance probability of $p = 5\%$.

There are clear similarities between Figure 4 and 5, but the extreme precipitation is found to increase over larger regions than the apparent HS in response to increased temperature consistent with earlier findings (Fischer et al. 2014; Pendergrass et al. 2015). For instance, regions such as the Mediterranean, which had a consistently negative HS, show increases in 20-year return values. Part of the subtropical ocean is the only common region with a decrease in both apparent HS and the 20-year return values. Note that the SO4x5, case unlike the other cases, gives a temperature reduction and hence a decrease in extreme precipitation.

Expected outcome of PDRMIP

PDRMIP aims to enhance the scientific understanding of how individual climate drivers cause changes to mean and extreme precipitation. The PDRMIP simulations will cast light on whether different climate driver abundances are a major source for the diversity in industrial era and future changes in precipitation among climate models by investigating the precipitation changes and their model diversity from several individual climate drivers. Since different drivers of climate change alter the atmospheric radiation budget in different ways, it is not obvious whether changes in mean and extreme precipitation events are similar among these drivers. PDRMIP has dedicated outputs and analyses to quantify extreme precipitation and other climate extremes from the different drivers of climate change.

Two studies, each using one climate model (Andrews et al. 2010; Kvalevåg et al. 2013) have demonstrated how both the fast and slow precipitation responses depend on atmospheric absorption and surface warming, for a range of drivers of climate change. PDRMIP will quantify the generality of these findings. Energy budget calculations enhance the understanding of climate model responses (Allen and Ingram 2002; Muller and O'Gorman 2011; Kravitz et al. 2013; Hodnebrog et al. 2016; Richardson et al. 2016) and such calculations will be performed within PDRMIP in order to understand precipitation and circulation changes from the different drivers. Since we include diagnostics (top of the atmosphere fluxes and surface temperature) that allow us to quantify radiative forcing in several ways (Boucher et al. 2013; Sherwood et al. 2015), PDRMIP will provide useful information on the methodology and uncertainties in radiative forcing calculations. The forcing analyses combined with energy budget analyses will provide information on the differences in the climate sensitivity among the PDRMIP climate drivers and models. Shindell (2014); Rotstayn et al. (2015); Shindell et al. (2015) found differences in the transient climate response (TCR) from inhomogeneous forcing agents. PDRMIP is a testbed for further understanding of these differences in TCR.

Recent climate model simulations show small surface temperature response to the current abundance of BC (Baker et al. 2015), but with relatively large inter-model variations. In PDRMIP a larger set of models will be applied with large BC perturbations and will include a number of forcing diagnostics. This will allow further analysis to better understand the finding of small surface temperature changes in Baker et al. (2015) and whether they arise from low climate sensitivity to BC or high importance of semi-direct effects (Koch and Del Genio 2010; Hodnebrog et al. 2014). This analysis will be linked to possible mitigation efforts, and additional simulations with regional pollution controls applied will be investigated in terms of precipitation impacts.

Summary

In PDRMIP, ten climate modelling groups have performed common idealized simulations to enhance our understanding of the impact of various climate drivers on precipitation. A core set of global perturbation simulations and additional regional perturbation simulations have already been performed with initial results presented in this study and Samset et al. (2016). PDRMIP consists of step-change experiments, but this process-based approach is highly valuable for understanding current and future precipitation changes. Precipitation changes are at the heart of two of the four questions related to the Grand Science Challenge on Clouds, Circulation and Climate Sensitivity (Bony et al. 2015) and frame many of the issues for the Grand Science Challenges on Water Availability (Trenberth and Asrar 2014) and Climate Extremes. The main PDRMIP results will be analysed during 2016-2018 to feed into the next IPCC Sixth Assessment Report (AR6). The main PDRMIP results will be updated on the website http://www.cicero.uio.no/en/PDRMIP with information on how to obtain model output which are publicly available. A description of available precipitation and energy budget relevant data is given at the web site. Finally, the web site has description of ongoing PDRMIP analysis and activities and we encourage further analysis based on the PDRMIP data to enhance understanding of diverse climate driver impact to the energy budget and precipitation.

Acknowledgement

PDRMIP is partly funded through the Norwegian Research Council project NAPEX (project number 229778). T. Takemura was supported by the supercomputer system of the National Institute for Environmental Studies, Japan, the Environment Research and Technology Development Fund (S-12-3) of the Ministry of the Environment, Japan and JSPS KAKENHI Grant Number 15H01728 and 15K12190. D. Olivie, A. Kirkevåg and T. Iversen were supported by the Norwegian Research Council through the projects EVA (grant 229771), EarthClim (207711/E10), NOTUR (nn2345k), and NorStore (ns2345k). M.Kasoar and A.Voulgarakis are supported by the Natural Environment Research Council under grant NE/K500872/1. Simulations with HadGEM3-GA4 were performed using the MONSooN system, a collaborative facility supplied under the Joint Weather and Climate Research Programme, which is a strategic partnership between the Met Office and the Natural Environment Research Council. TA was supported by the Joint UK DECC/Defra Met Office Hadley Centre Climate Programme (GA01101). We acknowledge the NASA High-End Computing Program through the NASA Center for Climate Simulation at Goddard Space Flight Center for computational resources to run the GISS-E2R model. O. Boucher acknowledges HPC resources from CCRT under the gencmip6 allocation provided by GENCI (Grand Equipement National de Calcul Intensif). T. Richardson and P. Forster were supported by NERC grants NE/K007483/1 and NE/N006038/1.

References

Allan RP, and Soden BJ, 2008: Atmospheric Warming and the Amplification of Precipitation Extremes. Science, 321, 1481–1484. [PubMed: 18687921]

Allan RP, Liu C, Zahn M, Lavers DA, Koukouvagias E, and Bodas-Salcedo A, 2014: Physically Consistent Responses of the Global Atmospheric Hydrological Cycle in Models and Observations. Surv. Geophys, 35, 533–552.

Allen MR, and Ingram WJ, 2002: Constraints on future changes in climate and the hydrologic cycle. Nature, 419, 224–232. [PubMed: 12226677]

Andrews T, Forster P, Boucher O, Bellouin N, and Jones A, 2010: Precipitation, radiative forcing and global temperature change. Geophys. Res. Lett, 37, L14701.

Arora VK, and Coauthors, 2011: Carbon emission limits required to satisfy future representative concentration pathways of greenhouse gases. Geophys. Res. Lett, 38, L05805.

Baker LH, Collins WJ, Olivié DJL, Cherian R, Hodnebrog Ø, Myhre G, and Quaas J, 2015: Climate responses to anthropogenic emissions of short-lived climate pollutants. Atmos. Chem. Phys, 15, 8201–8216.

Bala G, Caldeira K, and Nemani R, 2010: Fast versus slow response in climate change: implications for the global hydrological cycle. Climate Dynamics, 35, 423–434.

Ban N, Schmidli J, and Schär C, 2015: Heavy precipitation in a changing climate: Does short-term summer precipitation increase faster? Geophys. Res. Lett, 42, 1165–1172.

Bellouin N, Rae J, Jones A, Johnson C, Haywood J, and Boucher O, 2011: Aerosol forcing in the Climate Model Intercomparison Project (CMIP5) simulations by HadGEM2-ES and the role of ammonium nitrate. J. Geophys. Res.-Atmos, 116, D20206, 20210.21029/22011jd016074.

Bentsen M, and Coauthors, 2013: The Norwegian Earth System Model, NorESM1-M - Part 1: Description and basic evaluation of the physical climate. Geosci. Model Dev, 6, 687–720.

Berg P, Moseley C, and Haerter JO, 2013: Strong increase in convective precipitation in response to higher temperatures. Nature Geosci., 6, 181–185.

Bollasina MA, Ming Y, and Ramaswamy V, 2011: Anthropogenic Aerosols and the Weakening of the South Asian Summer Monsoon. Science, 334, 502–505. [PubMed: 21960529]

Bony S, Bellon G, Klocke D, Sherwood S, Fermepin S, and Denvil S, 2013: Robust direct effect of carbon dioxide on tropical circulation and regional precipitation. Nature Geosci, 6, 447–451.

Bony S, and Coauthors, 2015: Clouds, circulation and climate sensitivity. Nature Geosci, 8, 261–268.

Boucher O, and Coauthors, 2013: Clouds and Aerosols Climate Change 2013: The Physical Science Basis. Contribution of Working Group I to the Fifth Assessment Report of the Intergovernmental Panel on Climate Change, Stocker TF, and Coauthors, Eds., Cambridge University Press, Cambridge, United Kingdom and New York, NY, USA, 571–657.

Caesar J, and Lowe JA, 2012: Comparing the impacts of mitigation versus non-intervention scenarios on future temperature and precipitation extremes in the HadGEM2 climate model. J. Geophys. Res.-Atmos, 117, D15109.

Collins M, and Coauthors, 2013: Long-term Climate Change: Projections, Commitments and Irreversibility Climate Change 2013: The Physical Science Basis. Contribution of Working Group I to the Fifth Assessment Report of the Intergovernmental Panel on Climate Change, Stocker TF, Qin D, Plattner G-K, Tignor M, Allen SK, Boschung J, Nauels A, Xia Y, Bex V and Midgley PM, Ed., Cambridge University Press, 1029–1136.

Collins WJ, and Coauthors, 2011: Development and evaluation of an Earth-System model – HadGEM2. Geosci. Model Dev, 4, 1051–1075.

DeAngelis AM, Qu X, Zelinka MD, and Hall A, 2015: An observational radiative constraint on hydrologic cycle intensification. Nature, 528, 249–253. [PubMed: 26659186]

Dong B, Sutton RT, Highwood E, and Wilcox L, 2014: The Impacts of European and Asian Anthropogenic Sulfur Dioxide Emissions on Sahel Rainfall. J. Climate, 27, 7000–7017.

Dufresne J-L, and Coauthors, 2013: Climate change projections using the IPSL-CM5 Earth System Model: from CMIP3 to CMIP5. Clim. Dynam, 40, 2123–2165.

Ferraro A,J, and Griffiths GH, 2016: Quantifying the temperature-independent effect of stratospheric aerosol geoengineering on global-mean precipitation in a multi-model ensemble. Environ. Res. Lett, 11, 034012.

Fildier B, and Collins WD, 2015: Origins of climate model discrepancies in atmospheric shortwave absorption and global precipitation changes. Geophys. Res. Lett, 42, 8749–8757.

Fischer EM, Sedláček J, Hawkins E, and Knutti R, 2014: Models agree on forced response pattern of precipitation and temperature extremes. Geophys. Res. Lett, 41, 8554–8562.

Flato G, and Coauthors, 2013: Evaluation of Climate Models Climate Change 2013: The Physical Science Basis. Contribution of Working Group I to the Fifth Assessment Report of the Intergovernmental Panel on Climate Change, Stocker TF, and Coauthors, Eds., Cambridge University Press, 741–866.

Fläschner D, Mauritsen T, and Stevens B, 2016: Understanding the inter-model spread in global-mean hydrological sensitivity. J. Climate, 29, 801–817.

Forster P, and Coauthors, 2007: Changes in Atmospheric Constituents and in Radiative Forcing Climate Change 2007: The Physical Science Basis. Contribution of Working Group I to the Fourth Assessment Report of the Intergovernmental Panel on Climate Change, Cambridge University Press.

Frieler K, Meinshausen M, von Deimling TS, Andrews T, and Forster P, 2011: Changes in global-mean precipitation in response to warming, greenhouse gas forcing and black carbon. Geophys. Res. Lett, 38, L04702.

Gent PR, and Coauthors, 2011: The Community Climate System Model Version 4. J. Climate, 24, 4973–4991.

Gregory JM, and Coauthors, 2004: A new method for diagnosing radiative forcing and climate sensitivity. Geophys. Res. Lett, 31, L03205.

Hansen J, and Coauthors, 2005: Efficacy of climate forcings. J. Geophys. Res.-Atmos, 110, D18104, doi: 18110.11029/12005JD005776.

Held IM, and Soden BJ, 2006: Robust responses of the hydrological cycle to global warming. J. Climate, 19, 5686–5699.

Hodnebrog O, Myhre G, Forster PM, Sillmann J, and Samset BH, 2016: Local biomass burning is a dominant cause of the observed precipitation reduction in southern Africa. Nat Commun, 7, 11236. [PubMed: 27068129]

Hodnebrog Ø, Myhre G, and Samset BH, 2014: How shorter black carbon lifetime alters its climate effect. Nat Commun, 5, 5065. [PubMed: 25255429]

Hurrell JW, and Coauthors, 2013: The Community Earth System Model A Framework for Collaborative Research. Bull. Am. Meteorol. Soc, 94, 1339–1360.

Hwang Y-T, Frierson DMW, and Kang SM, 2013: Anthropogenic sulfate aerosol and the southward shift of tropical precipitation in the late 20th century. Geophys. Res. Lett, 40, 2845–2850.

Iversen T, and Coauthors, 2013: The Norwegian Earth System Model, NorESM1-M - Part 2: Climate response and scenario projections. Geoscl. Model Dev, 6, 389–415.

Kay JE, and Coauthors, 2015: THE COMMUNITY EARTH SYSTEM MODEL (CESM) LARGE ENSEMBLE PROJECT A Community Resource for Studying Climate Change in the Presence of Internal Climate Variability. Bull. Am. Meteorol. Soc, 96, 1333–1349.

Kendon EJ, Roberts NM, Fowler HJ, Roberts MJ, Chan SC, and Senior CA, 2014: Heavier summer downpours with climate change revealed by weather forecast resolution model. Nature Clim. Change, 4, 570–576.

Kharin VV, Zwiers FW, Zhang X, and Wehner M, 2013: Changes in temperature and precipitation extremes in the CMIP5 ensemble. Climatic Change, 119, 345–357.

Kirkevåg A, and Coauthors, 2013: Aerosol-climate interactions in the Norwegian Earth System Model-NorESM1-M. Geosci. Model Dev, 6, 207–244.

Knutti R, and Sedlacek J, 2013: Robustness and uncertainties in the new CMIP5 climate model projections. Nature Clim. Change, 3, 369–373.

Knutti R, Masson D, and Gettelman A, 2013: Climate model genealogy: Generation CMIP5 and how we got there. Geophys. Res. Lett, 40, 1194–1199.

Koch D, and Del Genio AD, 2010: Black carbon semi-direct effects on cloud cover: review and synthesis. Atmos. Chem. Phys, 10, 7685–7696.

Kravitz B, and Coauthors, 2013: An energetic perspective on hydrological cycle changes in the Geoengineering Model Intercomparison Project. J. Geophys. Res. - Atmos, 118, 13,087–013,102.

Kvalevåg MM, Samset BH, and Myhre G, 2013: Hydrological sensitivity to greenhouse gases and aerosols in a global climate model. Geophys. Res. Lett, 40, 1432–1438.

Lenderink G, and Van Meijgaard E, 2008: Increase in hourly precipitation extremes beyond expectations from temperature changes. Nature Geosci., 1, 511–514.

MacIntosh CR, Allan RP, Baker LH, Bellouin N, Collins W, Mousavi Z, and Shine KP, 2016: Contrasting fast precipitation responses to tropospheric and stratospheric ozone forcing. Geophys. Res. Lett, 43, 1263–1271.

Martin GM, and Coauthors, 2011: The HadGEM2 family of Met Office Unified Model climate configurations. Geosci. Model Dev, 4, 723–757.

Mehran A, AghaKouchak A, and Phillips TJ, 2014: Evaluation of CMIP5 continental precipitation simulations relative to satellite-based gauge-adjusted observations. J. Geophys. Res. - Atmos, 119, 1695–1707.

Merlis TM, 2015: Direct weakening of tropical circulations from masked CO2 radiative forcing. Proceedings of the National Academy of Sciences, 112, 13167–13171.

Ming Y, Ramaswamy V, and Persad G, 2010: Two opposing effects of absorbing aerosols on global-mean precipitation. Geophys. Res. Lett, 37, L13701.

Mitchell JFB, Wilson CA, and Cunnington WM, 1987: On CO_2 climate sensitivity and model dependence of results. Q. J. R. Meteorol. Soc, 113, 293–322.

Muller CJ, and O'Gorman PA, 2011: An energetic perspective on the regional response of precipitation to climate change. Nature Clim. Change, 1, 266–271.

Myhre G, and Coauthors, 2013a: Anthropogenic and Natural Radiative Forcing Climate Change 2013: The Physical Science Basis. Contribution of Working Group I to the Fifth Assessment Report of the Intergovernmental Panel on Climate Change, Stocker TF, and Coauthors, Eds., Cambridge University Press, Cambridge, United Kingdom and New York, NY, USA, 659–740.

Myhre G, and Coauthors, 2013b: Radiative forcing of the direct aerosol effect from AeroCom Phase II simulations. Atmos. Chem. Phys, 13, 1853–1877.

Neale RB, and Coauthors, 2010: Description of the NCAR Community Atmosphere Model (CAM 4.0), NCAR Technical Report, NCAR/TN-485+STR, National Center for Atmospheric Research (NCAR), Boulder, Colorado.

O'Gorman PA, Allan RP, Byrne MP, and Previdi M, 2012: Energetic Constraints on Precipitation Under Climate Change. Surv. Geophys, 33, 585–608.

O’Gorman P, 2015: Precipitation Extremes Under Climate Change. Curr Clim Change Rep, 1, 49–59. [PubMed: 26312211]

Otto-Bliesner BL, and Coauthors, 2015: Climate Variability and Change since 850 C.E.: An Ensemble Approach with the Community Earth System Model (CESM). Bull. Am. Meteorol. Soc

Pendergrass AG, and Hartmann DL, 2012: Global-mean precipitation and black carbon in AR4 simulations. Geophys. Res. Lett, 39, L01703.

Pendergrass AG, and Hartmann DL, 2014: The Atmospheric Energy Constraint on Global-Mean Precipitation Change. J. Climate, 27, 757–768.

Pendergrass AG, Lehner F, Sanderson BM, and Xu Y, 2015: Does extreme precipitation intensity depend on the emissions scenario? Geophys. Res. Lett, 42, 8767–8774.

Previdi M, 2010: Radiative feedbacks on global precipitation. Environ. Res. Lett, 5, 025211.

Richardson TB, Forster PM, Andrews T, and Parker DJ, 2016: Understanding the Rapid Precipitation Response to CO2 and Aerosol Forcing on a Regional Scale. J. Climate, 29, 583–594.

Rotstayn LD, Collier MA, Shindell DT, and Boucher O, 2015: Why Does Aerosol Forcing Control Historical Global-Mean Surface Temperature Change in CMIP5 Models? J. Climate, 28, 6608–6625.

Samset BH, and Coauthors, 2016: Fast and slow precipitation responses to individual climate forcers: A PDRMIP multimodel study. Geophys. Res. Lett, 43, 2782–2791.

Schmidt GA, and Coauthors, 2014: Configuration and assessment of the GISS ModelE2 contributions to the CMIP5 archive. J. Adv. Model. Earth Sy, 6, 141–184.

Shaw TA, and Voigt A, 2015: Tug of war on summertime circulation between radiative forcing and sea surface warming. Nature Geosci, 8, 560–566.

Sherwood SC, Bony S, Boucher O, Bretherton C, Forster PM, Gregory JM, and Stevens B, 2015: Adjustments in the Forcing-Feedback Framework for Understanding Climate Change. Bull. Am. Meteorol. Soc, 96, 217–228.

Shindell DT, 2014: Inhomogeneous forcing and transient climate sensitivity. Nature Clim. Change, 4, 274–277.

Shindell DT, Voulgarakis A, Faluvegi G, and Milly G, 2012: Precipitation response to regional radiative forcing. Atmos. Chem. Phys, 12, 6969–6982.

Shindell DT, Faluvegi G, Rotstayn L, and Milly G, 2015: Spatial patterns of radiative forcing and surface temperature response. J. Geophys. Res.-Atmos, 120, 5385–5403.

Sillmann J, Pozzoli L, Vignati E, Kloster S, and Feichter J, 2013a: Aerosol effect on climate extremes in Europe under different future scenarios. Geophys. Res. Lett, 40, 2290–2295.

Sillmann J, Kharin VV, Zwiers FW, Zhang X, and Bronaugh D, 2013b: Climate extremes indices in the CMIP5 multimodel ensemble: Part 2. Future climate projections. J. Geophys. Res.-Atmos, 118, 2473–2493.

Stephens GL, and Coauthors, 2012: An update on Earth's energy balance in light of the latest global observations. Nature Geosci, 5, 691–696.

Stier P, and Coauthors, 2013: Host model uncertainties in aerosol radiative forcing estimates: results from the AeroCom Prescribed intercomparison study. Atmos. Chem. Phys, 13, 3245–3270.

Stocker TF, and Coauthors, Eds., 2013: IPCC, 2013: Summary for Policymakers. Cambridge University Press, Cambridge, United Kingdom and New York, NY, USA, in press pp.

Takahashi K, 2009: The Global Hydrological Cycle and Atmospheric Shortwave Absorption in Climate Models under CO2 Forcing. J. Climate, 22, 5667–5675.

Takemura T, Nozawa T, Emori S, Nakajima TY, and Nakajima T, 2005: Simulation of climate response to aerosol direct and indirect effects with aerosol transport-radiation model. J. Geophys. Res.-Atmos, 110, D02202, doi:02210.01029/02004jd005029.

Takemura T, Egashira M, Matsuzawa K, Ichijo H, O'Ishi R, and Abe-Ouchi A, 2009: A simulation of the global distribution and radiative forcing of soil dust aerosols at the Last Glacial Maximum. Atmos. Chem. Phys, 9, 3061–3073.

Trenberth KE, 2011: Changes in precipitation with climate change. Climate Research, 47, 123–138.

Trenberth KE, and Asrar GR, 2014: Challenges and Opportunities in Water Cycle Research: WCRP Contributions. Surv. Geophys, 35, 515–532.

Walters DN, and Coauthors, 2014: The Met Office Unified Model Global Atmosphere 4.0 and JULES Global Land 4.0 configurations. Geosci. Model Dev, 7, 361–386.

Wasko C, Sharma A, and Westra S, 2016: Reduced spatial extent of extreme storms at higher temperatures. Geophys. Res. Lett, 43, 4026–4032.

Watanabe M, and Coauthors, 2010: Improved Climate Simulation by MIROC5: Mean States, Variability, and Climate Sensitivity. J. Climate, 23, 6312–6335.

Westra S, Alexander LV, and Zwiers FW, 2013: Global Increasing Trends in Annual Maximum Daily Precipitation. J. Climate, 26, 3904–3918.

Westra S, and Coauthors, 2014: Future changes to the intensity and frequency of short-duration extreme rainfall. Rev. Geophys, 52, 522–555.

Yoshimori M, and Broccoli AJ, 2008: Equilibrium Response of an Atmosphere–Mixed Layer Ocean Model to Different Radiative Forcing Agents: Global and Zonal Mean Response. J. Climate, 21, 4399–4423.

Box 1:

Precipitation changes and energy budget

The latent heat flux from evaporation and transpiration of water at the surface is compensated through the net condensation flux in the atmosphere. The global energy budget (at the top of the atmosphere, in the atmosphere and at the surface) is nearly in balance. Hence, the effect of a change in atmospheric composition on the energy budget is a useful framework for understanding the resulting changes in precipitation. In Box Figure 1, we break down the responses schematically, for three time scales: i) A perturbation may initially alter precipitation due to changes in the atmospheric radiative heating or cooling, which depends mainly on the radiative forcing agent. The change in atmospheric radiative cooling occurs more or less instantaneously. ii) Next, atmospheric temperature, clouds and water vapor are modified as a result of the changes in atmospheric radiative heating or cooling. These so-called rapid adjustments further alter precipitation. iii) Finally, precipitation is affected through climate feedback processes in response to the subsequent surface temperature changes, on time scales of years to decades.

Higher temperatures lead to increased atmospheric water vapor concentrations. Theoretical and model studies show that the global mean precipitation increases with global temperature change with a range of 1-3%/K (O'Gorman et al. 2012; Collins et al. 2013). Due to energetic constraints this is considerably smaller than the increase in vapor pressure, with temperature (6-7%/K) (Mitchell et al. 1987; Allen and Ingram 2002; O'Gorman et al. 2012; Allan et al. 2014; Pendergrass and Hartmann 2014). As shown in Box Figure 1, and introduced above, the energy budget of the troposphere must be approximately balanced. To first order; the global-mean atmospheric radiative cooling is balanced by latent heating through condensation and freezing minus re-evaporation of precipitation and sensible heat. Changes in atmospheric radiative cooling (due to the forcing agent itself or as a result of climate feedbacks) will therefore impact the release of latent heating and precipitation (Allen and Ingram 2002). This explains why the global mean precipitation changes do not simply scale with the amount of available water. Increased surface temperature and constant lapse rate enhances the atmospheric radiative cooling. For most drivers of climate change this is the dominant factor for precipitation changes (Andrews et al. 2010; Boucher et al. 2013; Samset et al. 2016). However, for the major driver of climate change, CO_2, the rapid adjustments cause a precipitation decrease that can significantly offset the increase driven by surface temperature increase.

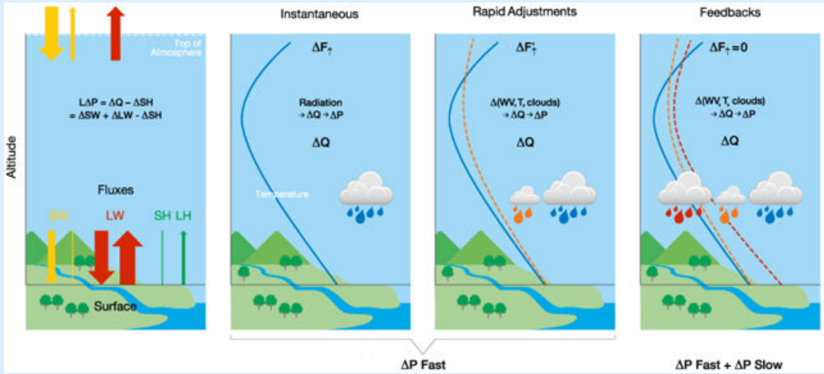

Box Figure 1:
Schematic diagram of the energy fluxes and fast and slow precipiation changes (ΔP) processes. Frame 1: At the top of the atmosphere, in the atmosphere and at the surface the energy budget is nearly in balance on a global scale. Changes in the atmospheric radiative cooling (ΔQ) can be caused by changes in absorption of shortwave radiation (SW) or changes in absorption/emission of longwave radiation (LW) or both. LH=LΔP is latent heat and SH is sensible heat. Frame 2: An external driver of climate change alters the radiative fluxes at the top of the atmosphere and this may alter the atmospheric absorption. Frame 3: The instantaneous change through radiation may further alter the atmospheric temperature, water vapor and clouds, through rapid adjustments. These rapid adjustments may lead to decrease or increase in clouds and water vapor and can vary through the atmosphere. The instantaneous radiative perturbation and rapid adjustments changes precipitation on a fast time scale (days to few years). Frame 4: Climate feedback processes through changes in the surface temperature further alter the atmospheric absorption which occurs on a long time scales (decades). Net radiative fluxes at the top of the atmosphere is given as F, water vapor as WV, temperature as T, and latent heat of vaporization L. In Frames 2 to 4, blue indicates the unperturbed state, orange represents the rapid adjustments and red represents the effect of both fast and slow adjustments.

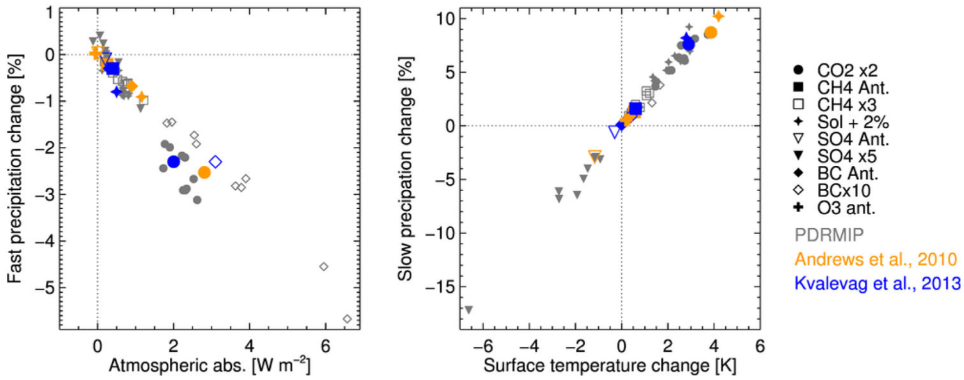

Figure 1:

Fast and slow global precipitation response as a function of atmospheric absorption and radiative forcing at the top of the atmosphere, respectively, from two modelling studies (Andrews et al. 2010; Kvalevåg et al. 2013) combined with PDRMIP results from Samset et al. (2016) as well as PDRMIP results from the IPSL-CM5A model. Ant in the legend denotes anthropogenic changes.

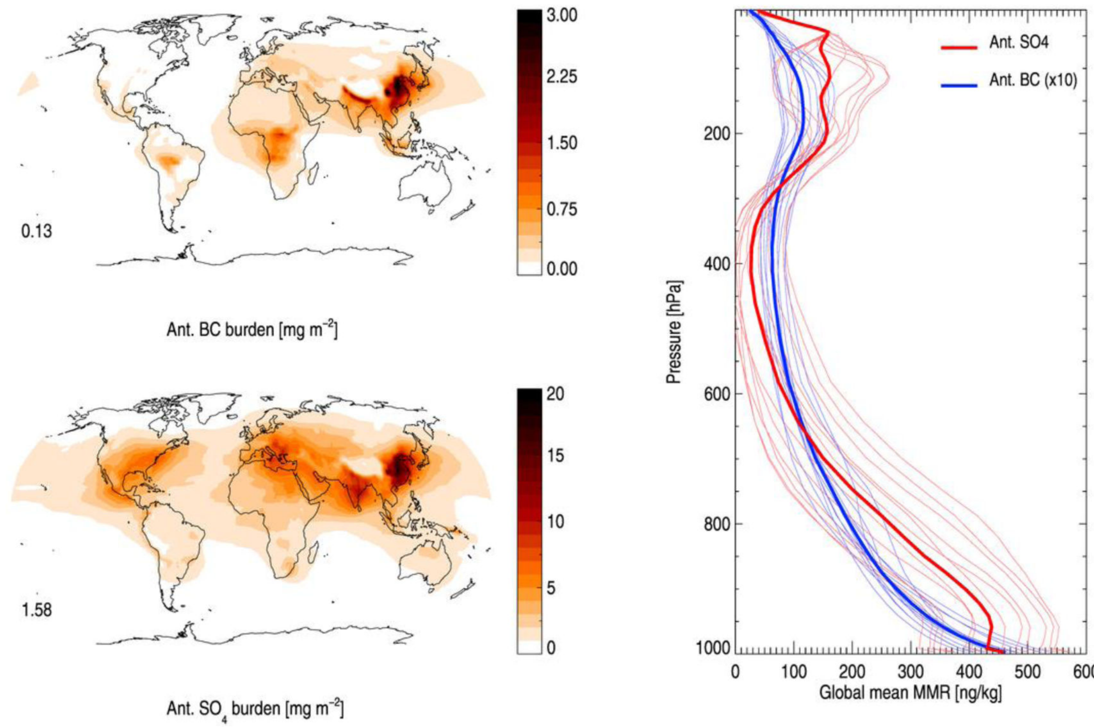

Figure 2:

PDRMIP prescribed anthropogenic burden and aerosol mass mixing ratio (MMR) fields, constructed from AeroCom Phase II models (Myhre et al. 2013b). The two left hand panels show the geographical distribution of the annual mean burden for BC (top) and SO4 (bottom) and (right hand panel) the vertical profile of MMR, of the present day increase in aerosol levels due to anthropogenic emissions. Thick lines show the annual means, thin lines show individual months for the vertical profiles. Note that BC MMR has been scaled by 10x for clarity.

NASA Author Manuscript
NASA Author Manuscript

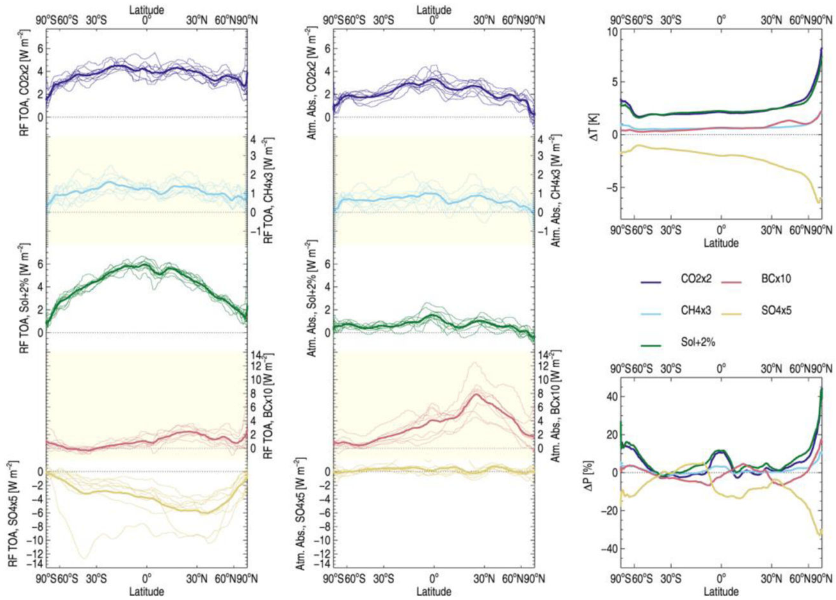

Figure 3:

Zonal and annual mean radiative forcing, atmospheric absorption, surface temperature change, and precipitation change for the five PDRMIP drivers. The left hand panel shows the zonal-annual mean top-of-atmosphere radiative forcing for the five PDRMIP drivers (from top bottom: CO_2 in blue, CH_4 in cyan, solar in green, BC in red and SO4 in yellow); the individual models are shown (thin lines), in addition to the multi-model mean (thick lines). The middle panel shows the same but for atmospheric absorption. The right hand panels show the surface temperature (top) and precipitation changes (bottom) for the multi-model mean for all five drivers (following the color coding from the left and centre panels). Radiative forcing and atmospheric absorption are diagnosed from the fixed-SST simulations.

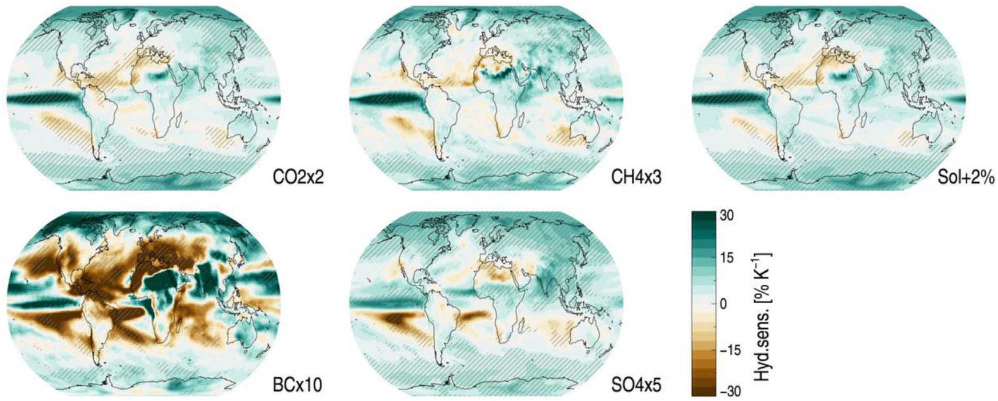

Figure 4:
Geographical distribution of multi-model mean apparent HS parameter for the five PDRMIP drivers experiments (CO2x2, CH4x3, Solar+2%, BCx10, SO4x5). The apparent HS is calculated as annual mean geographical precipitation change divided by global and annual mean temperature change relative to the base simulation. The hatching is included where the mean apparent HS over the 50 years period is more than one standard deviation away from zero.

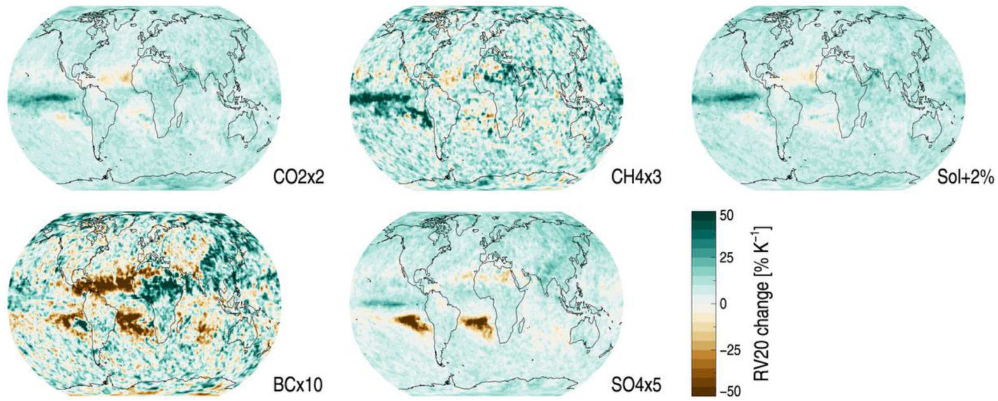

Figure 5:

Geographical distribution of multi-model mean changes in 20-year return values of annual maximum daily precipitation per unit of global warming for the five PDRMIP driver experiments (CO2x2, CH4x3, Solar+2%, BCx10, SO4x5). The change in 20-year return values is given as percentage change divided by global and annual mean temperature change relative to the base simulation.

NASA Author Manuscript

NASA Author Manuscript

Table 1:

PDRMIP core experiments. All experiments are performed with both fixed-SST (a minimum of 15 years) and coupled model configurations (100 years).

Name	Description
Base	Specified all anthropogenic and natural climate forcing agents at present day abundances (preferred) or pre-industrial abundances
CO_2 x 2	Doubling of the CO_2 concentration relative to **Base**
CH_4 x 3	Tripling of the CH_4 concentration relative to **Base**
Solar+2%	Total solar irradiance is increased by 2%
Sul x 5	Increase the anthropogenic sulphate concentration or emissions by 5 times relative to **Base**
BC x 10	Increase the anthropogenic BC concentration or emissions 10 times relative to **Base**

Table 2:

PDRMIP additional experiments. All experiments are performed with both fixed-SST and coupled model configurations. The European region is defined for longitudes between 10°W and 40°E and latitudes between 35°N and 70°N. Likewise the region of Asia is defined for longitudes between 60°E and 140°E and latitudes between 10°N and 50°N.

Name	Description
Sulred	Sulphate concentration from present day concentration to preindustrial concentration
Suleur	Sulphate present day anthropogenic concentration multiplied by 10, Europe only
Sulasia	Sulphate present day anthropogenic concentration multiplied by 10, Asia only
BCasia	Black carbon present day anthropogenic concentration multiplied by 10, Asia only
Sulasiared	Similar to Sulred, but Asia only
O3asia	Increase in ozone, Asia only, comparable forcing to Sulasia

Table 3:

Description of the ten PDRMIP models.

Model	Version	Resolution	Ocean setup	Aerosol setup	Key references
CanESM2	2010	2.8°x2.8°, 35 levels	Coupled ocean	Emissions	(Arora et al. 2011)
NCAR-CESM1-CAM4	1.0.3	2.5°x1.9°, 26 levels	Slab ocean	Fixed concentrations	(Neale et al. 2010; Gent et al. 2011)
NCAR-CESM1-CAM5	1.1.2	2.5°x1.9°, 30 levels	Coupled ocean	Emissions	(Hurrell et al. 2013). This is the same model as (Kay et al. 2015), but with a coarser resolution (Otto-Bliesner et al. 2015)
GISS-E2-R	E2-R	2°x2.5°, 40 levels	Coupled ocean	Fixed concentrations	(Schmidt et al. 2014)
HadGEM2-ES	6.6.3	1.875°x1.2 5°, 38 levels	Coupled ocean	Emissions	(Collins et al. 2011; Martin et al. 2011)
HadGEM3	GA 4.0	1.875°x1.2 5°, 85 levels	Coupled ocean	Fixed concentrations	(Bellouin et al. 2011; Walters et al. 2014)
IPSL-CM5A	CMIP5	3.75°x 1.875°, 39 levels	Coupled ocean	Fixed concentrations	(Dufresne et al. 2013)
MPI-ESM	1.1.00p2	T63, 47 levels	Coupled ocean	Climatology, year 2000	Roeckner et al. 2016 (in prep.)
NorESM1	NorESM1-M	2.5°x1.9°, 26 levels	Coupled ocean	Fixed concentrations	(Bentsen et al. 2013; Iversen et al. 2013; Kirkevåg et al. 2013)
MIROC-SPRINTARS	5.9.0	T85 (approx.. 1.4°x1.4°), 40 levels	Coupled ocean	HTAP2 emissions	(Takemura et al. 2005; Takemura et al. 2009; Watanabe et al. 2010)